Evolution of the subglacial hydrologic system beneath the rapidly decaying Cordilleran Ice Sheet caused by ice-dammed lake drainage: implications for meltwater-induced ice acceleration

Matthew J. Burke*, Tracy A. Brennand, Andrew J. Perkins

Department of Geography, Simon Fraser University, Burnaby, BC V5A 1S6, Canada

ARTICLE INFO

ABSTRACT

A positive correlation between ice-dammed lake drainage and ice acceleration at Antarctic Ice Sheets (AIS) and land-terminating sections of the Greenland Ice Sheet (GrIS) has been implicated in enhanced ice sheet decay. However, the paucity of direct measurements at the ice sheet bed restricts our understanding of subglacial drainage system evolution in response to transient water inputs. We present evidence that two meltwater corridors on the former bed of the thin (~600 m at Last Glacial Maximum over the interior Plateaus of British Columbia) and rapidly decaying Cordilleran Ice Sheet (CIS) were generated subglacially in response to the drainage of an ice-dammed lake and operated as canals (tunnel channels). Geomorphological, ground-penetrating radar (GPR) and electrical resistivity tomography (ERT) data reveal a simple event sequence that includes initial propagation of a broad (at least 2.5 km wide) floodwave (inefficient drainage) from an ice-dammed lake, over relatively short (3–24 km) zones at the corridor heads that collapsed into efficient canals (large (up to 0.25–2.5 km wide) channels incised down into the sediment bed and up into the ice) downglacier. Canal formation on the southern Fraser Plateau involved synchronous (along the full canal length) system development, including elements of headward erosion and plunge pool formation. Our data suggest that ice-dammed lake drainage beneath a rapidly decaying thin ice mass that has an efficient antecedent drainage network is not conducive to large-scale ice acceleration. These data may aid better assessment of the role of ice-dammed lake drainage on the dynamics of former, as well as contemporary, ice sheets.

© 2012 Elsevier Ltd. All rights reserved.

1. Introduction

Evidence of transient hydrological systems at the Antarctic (AIS) and Greenland (GrIS) Ice Sheets is challenging the traditional assumption that subglacial hydrodynamics of large ice sheets are steady-state (e.g., Gray et al., 2005; Wingham et al., 2006; Bell, 2008; Stearns et al., 2008; Carter et al., 2009; Jordan et al., 2010; Palmer et al., 2011). For the large ice streams and outlet glaciers of the AIS and GrIS the influence of subglacial water on fast ice flow depends on the hydrologic system (Bell, 2008). Water flow through a well-connected efficient drainage network will have little impact on ice velocity, whereas water flow through an inefficient, spatially-distributed network can reduce effective pressure at the ice-bed interface, triggering ice acceleration (Bell, 2008; Bartholemew et al., 2011; Sundal et al., 2011). Thus, the supply

and distribution of subglacial water can modulate ice dynamics (Bell, 2008).

Unlike the AIS, the GrIS has extensive areas of surface melt that can drain into the subglacial hydrologic system either directly, through crevasses and moulins, or following temporary storage in subglacial lakes (Bell, 2008). A positive correlation between surface melting and seasonal ice sheet acceleration has been identified for the GrIS, suggesting that an increased influx of supraglacial water induces ice acceleration (Zwally et al., 2002; Bartholemew et al., 2010, 2011; Palmer et al., 2011). During the ablation season, surface melt lakes up to several kilometres in diameter develop near the ice sheet margin and can enlarge quickly (Box and Ski, 2007; McMillan et al., 2007). The sudden drainage of these lakes to the bed due to hydro-fracture propagation (Krawczynski et al., 2009) can result in temporary subglacial water storage, ice uplift and acceleration, followed by channelized drainage (Zwally et al., 2002; Das et al., 2008; Sole et al., 2011). Although the AIS does not have extensive areas of supraglacial melt, 387 subglacial lakes have so far been identified (Wright and Siegert, 2011). Recent

* Corresponding author. Tel.: +1 778 782 3823; fax: +1 778 782 5841.
  E-mail address: mjburke@sfu.ca (M.J. Burke).

observations have shown a number of subglacial lakes to be dynamic, with large volumes of water moving between lakes (e.g., Gray et al., 2005; Wingham et al., 2006; Fricker et al., 2007; Fricker and Scambos, 2009) and to the ice sheet margin (e.g., Goodwin, 1988). Such water movement has been linked to ice acceleration (e.g., Stearns et al., 2008). Although ice sheet models require quantification of the hydrodynamics operating at the ice-bed interface, difficulties in directly accessing the ice-bed interface prevent direct measurements of hydrological system response during ice-dammed lake drainage.

The detailed analysis of glaciofluvial landforms at former ice sheet beds present an opportunity to elucidate hydrological processes operating beneath decaying ice sheets. Tunnel channels (or tunnel valleys) are the erosive expression of channelized subglacial water flows, whereas meltwater channels (typically smaller than tunnel channels/valleys) usually record ice-marginal or proglacial flow. Tunnel channels/valleys are elongate troughs cut into sediment or bedrock that may be up to 100 km long and 4 km wide (Ó Cofaigh, 1996; Russell et al., 2007). Where they are inferred to have formed by bankfull flow they are called tunnel channels (e.g., Brennand and Shaw, 1994; Fisher et al., 2005), whereas those thought to have formed under less than bankfull flow conditions are named tunnel valleys (e.g., Wright, 1973; Mooers, 1989). In either case, tunnel channel/valley walls may be discontinuous and so partly ice-walled during formation (e.g., Shaw, 1983; Rampton, 2000; Utting et al., 2009). They often truncate subglacial bedforms and/or till, have long upslope segments, and contain depositional landforms such as eskers and gravel dunes (Shaw and Gorrell, 1991; Brennand and Shaw, 1994; Ó Cofaigh, 1996; Fisher et al., 2005). However, there is much controversy surrounding the magnitude and frequency of these flows (Ó Cofaigh, 1996). Broadly speaking, there are four main hypotheses of tunnel channel/valley formation:

1) Headward tunnel valley growth by steady-state subglacial sediment deformation into a laterally migrating R-channel that was initiated by piping (e.g., Boulton and Hindmarsh, 1987). Glaciofluvial erosion of substrate material squeezed into the steady-state R-channel allowed the enlargement of tunnel valleys over a prolonged period of time.
2) Synchronous occupation and incision of the entire tunnel channel system by catastrophic subglacial outburst floods (e.g., Wright, 1973; Shaw and Gorrell, 1991; Brennand and Shaw, 1994; Sjogren et al., 2002).
3) Time-transgressive tunnel valley development via catastrophic drainage of subglacial lakes close to a retreating ice margin (Wingfield, 1990). Tunnel channel segments underwent headward erosion via plunge pool incision and tunnel valleys formed time-transgressively with ice retreat. Each segment was eroded by a separate outburst flood.
4) Seasonal formation of tunnel valley segments close to the ice margin from water supplied by supraglacial melting (Mooers, 1989). Ice retreat and continued segment erosion formed tunnel valleys time-transgressively.

As interpretations of tunnel channel/valley formation aid reconstruction of Late Wisconsinan ice sheet hydrology and dynamics, it is important to fully understand the mechanisms responsible for their development (Brennand et al., 2006). Tunnel channels/valleys in Canada are often inferred to have developed during single events (e.g., Shaw, 1983; Brennand and Shaw, 1994), whereas evidence from some European tunnel channels/valleys suggest palimpsest development over multiple glaciations (e.g., Jørgensen and Sandersen, 2008). Significant insight into the past meltwater regime within a tunnel channel/valley can be gained

from analysis of channel/valley fill (e.g., Shaw and Gorrell, 1991; Piotrowski, 1994; Russell et al., 2003; Fisher et al., 2005; Jørgensen and Sandersen, 2008; Lang et al., 2012). The sedimentary structure and architecture of tunnel channel/valley fills have been described on the basis of their geomorphology, sedimentary exposures (e.g., Shaw and Gorrell, 1991), and from geophysics (e.g., Pugin et al., 1999; Fisher et al., 2005). Tunnel channels/valleys are often filled, partially or completely, with sand and gravel that is typically arranged into bedforms or hummocks (e.g., Shaw and Gorrell, 1991; Piotrowski, 1994; Russell et al., 2003; Fisher et al., 2005; Utting et al., 2009), tabular sheets (e.g., Pugin et al., 1999; Russell et al., 2003) and eskers (e.g., Shaw, 1983; Brennand and Shaw, 1994; Ó Cofaigh, 1996; Fisher et al., 2005). Eskers record the infilling of ice tunnels that may form supraglacially, englacially or subglacially (Brennand, 1994). Because tunnel channels/valleys often contain eskers, it has been suggested that eskers may record waning stage deposition following tunnel channel/valley incision by high-magnitude, bankfull flow (Shaw, 1983). Alternatively, eskers may record a later depositional phase, unrelated to tunnel channel/valley incision. Recent jökulhlaups at contemporary glaciers are known to have produced both eskers (Burke et al., 2008, 2010) and tunnel channels (Russell et al., 2007).

To-date most Canadian work has focused on Laurentide Ice Sheet (LIS) tunnel channels/valleys (e.g., Sjogren et al., 2002; Russell et al., 2003). We have limited knowledge of tunnel channels/valleys formed under the Cordilleran Ice Sheet (CIS) (e.g., Booth and Hallet, 1993; Booth, 1994; Lesemann and Brennand, 2009). In this paper we investigate the morphology and fill of two meltwater corridors (tunnel channels/valleys) on the southern Fraser Plateau, British Columbia (BC), Canada (we use the term meltwater corridor as the landform does not have continuous valley walls and includes both erosional and depositional elements). These corridors give detailed insight into subglacial drainage system evolution beneath a thin ice sheet (CIS was only ~600 m thick on the interior plateaus of BC at Last Glacial Maximum (LGM); cf. Huntley and Broster, 1994) in response to ice-dammed lake drainage. These data allow us to assess the mode of meltwater corridor formation beneath the CIS and may improve assessment of the significance of ice-dammed lake drainage on the dynamics of former, as well as contemporary ice sheets.

2. Depositional setting

The southern Fraser Plateau, located in the intermontane region of BC, Canada, is dissected near its southern margin by the ~200–300 m deep Bonaparte Valley (Fig. 1). The relatively flat topography of the plateau is controlled by the 10–50 m thick basalt flows (Chilcotin group; 10–7 Ma) (Andrews et al., 2011) that sit atop a complex of granitic and metamorphic basement rocks (Plouffe et al., 2011). Faulting is rare within the basalt (Campbell and Tipper, 1971), but contemporary drainage patterns are controlled by antecedent, broad undulations (trending northwest to southeast) in the plateau surface, attributed to regional scale warping (Mathews, 1989) during prolonged uplift in the Neogene (Andrews et al., 2009). The bedrock plateau surface is largely covered in a thin (~1–15 m thick) single layer of till, that is streamlined in places (Plouffe et al., 2011). This till lies stratigraphically above lake sediments deposited after $\delta^{18}O$ stage 4 (59–74 ka) (Lian and Hicock, 2001) and is generally associated with drift deposited during the last glaciation (cf. Fulton and Smith, 1978). Consequently, till on the plateau was most likely deposited during the last glaciation of BC (cf. Huntley and Broster, 1994, 1996; Lian and Hicock, 2000, 2001; Plouffe et al., 2011).

Growth of the last CIS in BC began around 30.5 cal ka BP (Booth et al., 2003), and is thought to have become cold-based as it
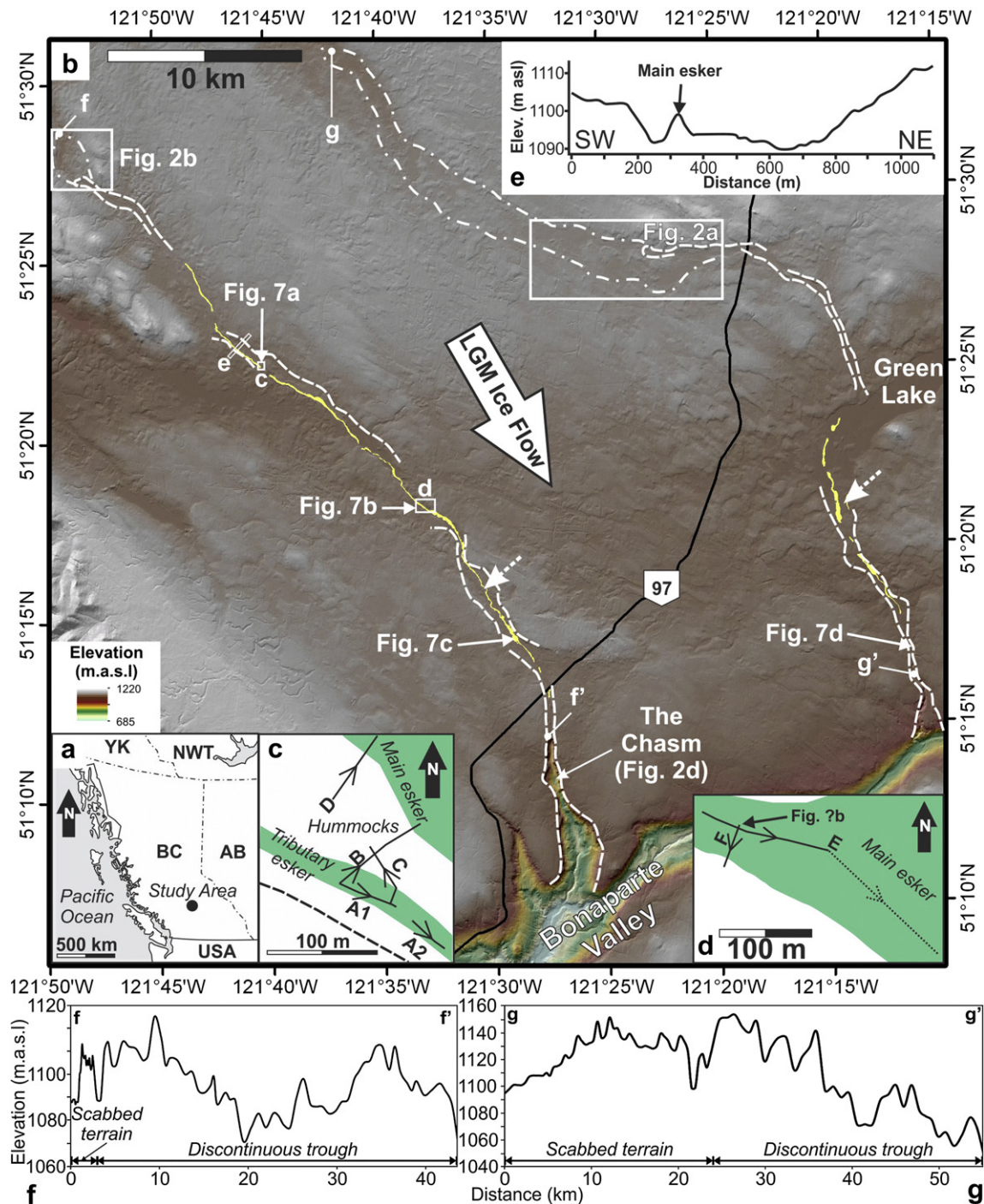
Fig. 1. a) The location of the study area (southern Fraser Plateau) is indicated by the labelled black dot in British Columbia (BC). b) A hillshaded elevation model of the southern Fraser Plateau (Geobase®). The dashed white lines and dot-dashed lines highlight the discontinuous troughs (downglacier section) and scabbed terrain (upglacier section) of the meltwater corridors, respectively; the yellow lines are the eskers. The boxes labelled "c–e" indicate the location of the panels shown in c)–e) and the dashed arrows show the location of possible hummocks similar to those at c). The boxes and arrows labelled Fig. 2a, b, d and Fig. 6a–d show the location of panels in the corresponding Figures. The large labelled white arrow indicates ice flow direction at last glacial maximum (LGM) (cf. Plouffe et al., 2011). f–f' and g–g' correspond to up- and downflow ends of the elevation profiles presented in f) and g). Maps of geophysical survey lines at c) grid 1 and d) grid 2. Solid lines indicate GPR lines alone, whereas the dotted line indicates both GPR and ERT lines. Survey direction is indicated by the arrows. The dashed line is the wall of the meltwater corridor. The green areas show the relative positions of eskers. Elevation profiles e) across the Chasm discontinuous trough, f) along the Chasm meltwater corridor axis, and g) along the Green Lake meltwater corridor axis. (For interpretation of the references to colour in this figure legend, the reader is referred to the web version of this article.)

expanded over the Fraser Plateau, as inferred from glaciotectonic structures in bedrock and sub-till sediments (Lian and Hicock, 2000). Ice advanced onto the Fraser Plateau from the Cariboo Mountains in the east (Plouffe et al., 2011) and the Coast Mountains in the west (Huntley and Broster, 1996; Clague and James, 2002),

but was forced to flow northwest and southeast at the junction between westward- and eastward-flowing ice (Huntley and Broster, 1996; Clague and James, 2002). The CIS reached its maximum at around 14–13 cal ka BP when the southern Fraser Plateau was covered by ice ∼600 m thick (Huntley and Broster,

1994), as recorded by the maximum elevation of glacial trimlines and minimum elevations of relict periglacial landforms (Huntley and Broster, 1996). Due to increased ice thickness and, thus, pore-water pressure, the initially cold-based CIS, is thought to have shifted to a temperate thermal regime (Lian and Hicock, 2000). Rapid decay of the southern sector of the CIS, from southeast to northwest (Plouffe et al., 2011), was complete by 10.7 cal ka BP (Clague and James, 2002) and is recorded by meltwater channels, eskers, outwash sediments, hummocky deposits, and glaciolacustrine sediments. There is a distinct lack of large recessional moraines on the interior plateaus of BC (cf. Tipper, 1971), and Fulton (1991) ascribes this to ice stagnation and downwasting. Although large moraines are absent, there are a number of meltwater landforms that can give insight into the dynamics and hydrology of the decaying CIS. The most prominent of these are two large meltwater corridors northwest of the Bonaparte Valley at The Chasm and Green Lake (Fig. 1).

3. Methods

3.1. Landform mapping and geophysical data collection

The geomorphology of the Chasm and Green Lake meltwater corridors were mapped using stereographic aerial photographs (1:40 000) and small-scale digital elevation models (DEMs; 25 m horizontal resolution, 10 m vertical resolution, Geobase®). Because sediment sections are rare on the Fraser Plateau, shallow geophysical techniques were employed to investigate the sedimentary architecture of the Chasm meltwater corridor fill. A total of 680 m of 100 MHz common offset (CO) ground-penetrating radar (GPR) lines were collected as two grids (Fig. 1c, d) within the Chasm meltwater corridor using a Sensors & Software Inc. pulseEKKO PRO system. The presence of tree stumps and slash within the clear cut (an area recently deforested by logging) at grid 1 (Fig. 1c) prevented collection of regularly spaced lines. During CO data collection, the GPR antennas were co-polarised and perpendicular-broadside to the survey line, to reduce reflections from offline sources (Arcone et al., 1995). Antennas were kept at a constant separation of 1 m and data were collected in step mode (0.25 m) along the lines to improve ground coupling and trace stacking (32 traces). Seven common mid-point (CMP) profiles, collected on the esker at grids 1 and 2, provide an estimated subsurface average velocity of 0.121 ± 0.008 m/ns, which was used to convert two-way travel time (TWT) into depth and for data processing. At grid 2 (Fig. 1d), a 165 m long electrical resistivity tomography (ERT) line was also collected using an eight channel Advanced Geosciences Inc. (AGI) Super Sting system. Data were collected as a dipole–dipole survey with 1.5 m electrode spacing. All GPR and ERT lines were surveyed for topographic variation using a real-time kinematic differential global positioning system (dGPS).

3.2. Geophysical data processing and inversion

GPR data processing was carried out in REFLEXW v5.6 and included static correction, 'dewow' filtering, bandpass filtering, migration, background removal filtering, application of a gain function, and topographic correction. ERT inversion was carried out in AGI EarthImager 2D v2.40 using the finite element method as a forward model, a smooth model inversion routine, damped transform topographic correction, removal of negative resistivity values and spikes, a minimum voltage filter, and minimum and maximum apparent resistivity filters. Inversion resulted in a total of 8% data removal, a maximum RMS error of 3.10% and an l^2 value (squared and summed differences between apparent and actual resistivity values) of <2.5.

4. Results and interpretation

4.1. Meltwater corridor landsystem

Two prominent, northwest to southeast orientated (similar to LGM ice flow direction, cf. Plouffe et al., 2011) meltwater corridors (spaced ∼10–15 km) on the southern Fraser Plateau, BC (Fig. 1) terminate in large bedrock cataracts (with plunge pools at their heads) that were carved in a headward fashion from the Bonaparte valley. The Chasm bedrock cataract (Fig. 2d) is ∼6 km long, ∼0.5–1.5 km wide, and ∼0.1–0.3 km deep, whereas that south of Green Lake is smaller at ∼3.5 km long, ∼0.3–0.6 km wide, and ∼0.05–0.1 km deep. The meltwater corridor upflow from the Chasm is ∼45 km long and ∼0.25–2.5 km wide, whereas the Green Lake corridor is ∼55 km long (upflow from its bedrock cataract) and 0.1–2.5 km wide. The meltwater corridors are relatively straight (sinuosity values of 1.05 and 1.1 for the Chasm and Green Lake respectively, defined by the ratio between channel and straight line length) and have undulating long profiles that include significant upslope segments (Fig. 1f, g). They can be split into upglacier and downglacier sections based upon abrupt changes in morphology (Fig. 1b, f and g). Downglacier sections of the meltwater corridors are defined by discontinuous (and not always well-defined) troughs irregularly cut (up to 20 m deep, Fig. 1e) into the underlying substrate (till and/or bedrock) (Fig. 1b). The trough north of the Chasm is ∼42 km long and ∼0.25–1 km wide and that at Green Lake is ∼30 km long and 0.1–2.5 km wide. The trough heads are defined by abrupt, ∼0.5 km wide and >10 m deep (relative to lake surfaces) basins (recessional cataracts) forming plunge pools that have double horseshoe planforms (Fig. 2a, b). The upglacier sections of the meltwater corridors are composed of broad (up to 2.5 km wide) zones of scabbed terrain that include erosional remnants aligned with the corridor axes (Fig. 2a–c). The scabbed terrain at the Chasm is ∼3 km long, whereas that at Green Lake is ∼24 km long. These broad zones of scabbed terrain terminate abruptly <3 km downglacier of the horseshoe-shaped basins that define the heads of the discontinuous troughs. The discontinuous troughs contain eskers (up to 20 m high and ∼20–300 m wide) along most of their length and the eskers drape hummocks that occur within corridor widenings (Fig 1 and Fig 3a–d). The hummocks have crestlines oblique (though variably orientated) to the corridor axis (Fig. 3a–c).

Similar discontinuous meltwater corridors (spaced ∼3–10 km apart) have been identified elsewhere and are thought to record subglacial water flow (Shaw, 1983; Rampton, 2000; Utting et al., 2009). Because the meltwater corridors on the Fraser Plateau have a low sinuosity, undulating long profiles with long up-slope segments, till and bedrock walls, and contain eskers, we interpret them as tunnel channels/valleys (Brennand and Shaw, 1994; Russell et al., 2003; Fisher et al., 2005).

4.2. Meltwater corridor fill characteristics

GPR data provide information on subsurface architecture (Neal, 2004), whereas ERT measures variations in resistivity that are primarily controlled by grain size (porosity) and water content (Van Dam, 2012). Radar bounding surfaces (labelled R1–R24 in Figs. 4 and 5) are high amplitude, continuous reflections that can be traced across multiple GPR profiles and demarcate the termination of reflections above and below. These bounding surfaces define 26 radar elements (RE) within the fill that can be grouped into four stratigraphic element associations (Table 1): 1) corridor substrate; 2) broad corridor fill elements; 3) esker elements; and 4) post glacial elements.
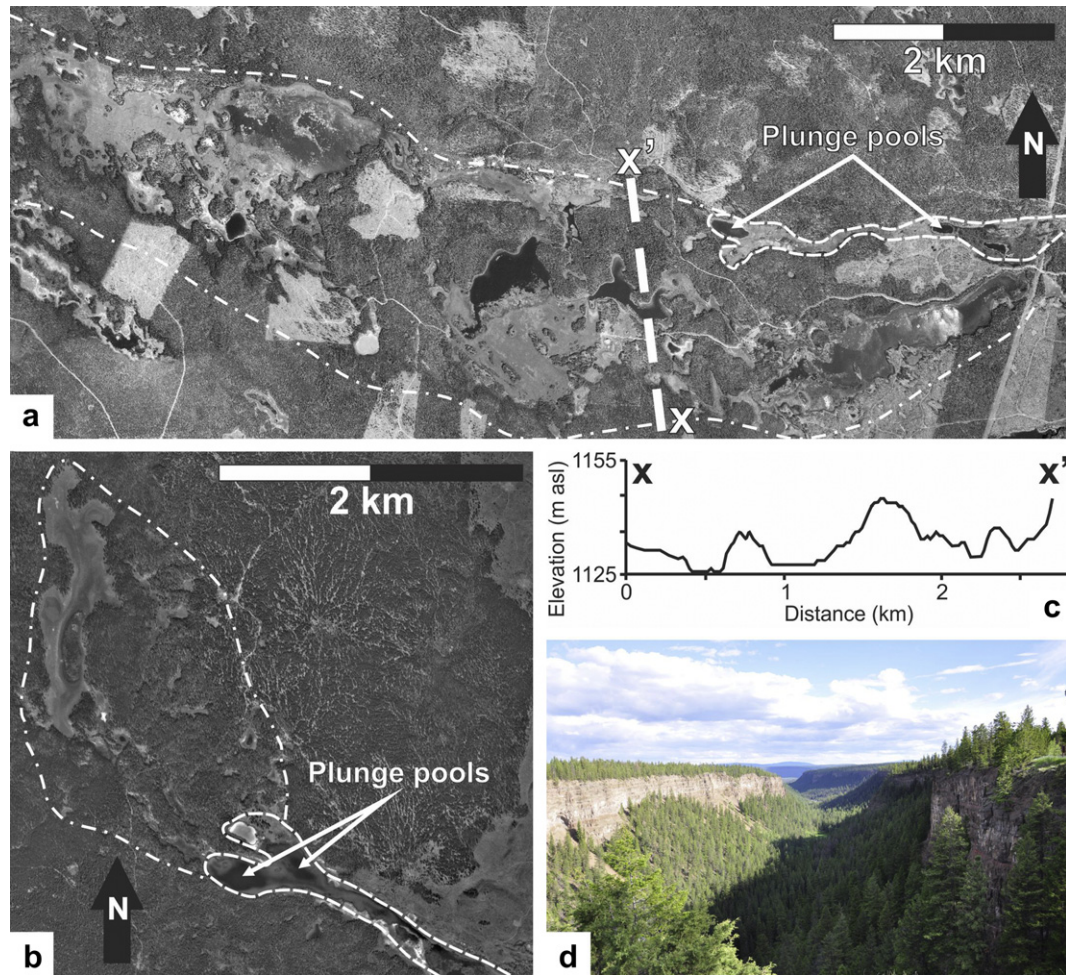
Fig. 2. a) Orthophotograph (Province of British Columbia, 2010) showing part of the scabbed terrain (dot-dashed line) and head of the discontinuous trough (dashed line) along the Green Lake meltwater corridor (refer to Fig. 1b for location). x–x′ corresponds to the start and end points of the elevation profile in c). b) Orthophotograph (Province of British Columbia, 2010) showing the scabbed terrain (dot-dashed line) and the head of the discontinuous trough (dashed line) along the Chasm meltwater corridor (see Fig. 1b for location). c) Elevation profile across the Green Lake meltwater corridor scabbed terrain. d) Photograph looking downflow from the head of the Chasm bedrock cataract. Here the cataract is ∼500 m wide and 100–200 m deep.

4.2.1. Corridor substrate (RE-A)

RE-A is identified throughout most of grid 1 (Fig. 4) and grid 2 (Fig. 5), though no lower bounding surface is imaged due to rapid signal attenuation that is independent of GPR system electronics. RE-A is largely reflection free, it has an irregular upper bounding surface, and ERT data (Fig. 5b) show it corresponds to an order-of-magnitude resistivity transition (from ∼1500–13,000 Ω-m above R1 to ∼9–400 Ω-m below R1, Fig. 5d).

Interpretation: RE-A is interpreted as till because: 1) it is reflection free; 2) its upper bounding surface is not flat (as expected for a water table); 3) the signal rapidly attenuates within it (Fig. 4c–e and Fig. 5b); and 4) the measured resistivity (9–400 Ohm-m) is similar to resistivity values of till measured elsewhere on the southern Fraser Plateau. This interpretation is consistent with the characteristics of till identified in other GPR surveys (Beres and Haeni, 1991; Pugin et al., 1999; Ékes and Hickin, 2001). Consequently, RE-A corresponds to the corridor substrate, which is composed of till at the GPR grids. In some other places the meltwater corridors are at least partially walled by bedrock.

4.2.2. Broad corridor fill elements: gravel sheets and gravel dunes (RE-B to RE-J)

The high resistivity (∼1500–13,000 Ω-m, Fig. 5b, d) of material above RE-A corresponds to good GPR signal penetration through those radar elements that correspond to the corridor fill. The lowest corridor fill element, RE-B, is identified at grids 1 and 2, and has a sheet-like geometry (orange, Fig. 4h–j, 5d). Internal reflections are moderately continuous and subparallel to the lower bounding surface (R1) onto which they are either draped (e.g., at ∼20–85 m on line B, Fig. 4h) or onlapped (e.g., at ∼6–13 m on line C, Fig. 4i). Subsequent corridor fill is recorded by eight lenticular, convex-up and stacked radar elements, which have lower bounding surfaces that truncate deeper reflections (RE-C to RE-J; yellow, Fig. 4). These radar elements form stacked hummocks at grid 1 and conform to hummocks at the ground surface (e.g., 1 and 2, Fig. 3b, c and Fig. 4). The hummocks have ground expressions up to 4 m high and have 38 m long crestlines that are roughly aligned northeast to southwest. The hummocks are draped onto RE-B throughout most of grid 1, except at the south-western side (Fig. 4e–i) where they are draped directly onto till (RE-A). Internally these stacked radar elements have convex-up, concave-up, and pseudo-planar reflection geometries in various line orientations. Where GPR profiles are close to perpendicular (no GPR lines were exactly perpendicular) to the hummock crestline (e.g., RE-G, RE-I, RE-J, Fig. 4h) reflections that dip ∼15° towards the northeast (this is an apparent dip because GPR line B was oblique to hummock crestline) are identified. Dipping reflections are not clearly identified in RE-C to RE-F and RE-H presumably because the GPR line is not perpendicular
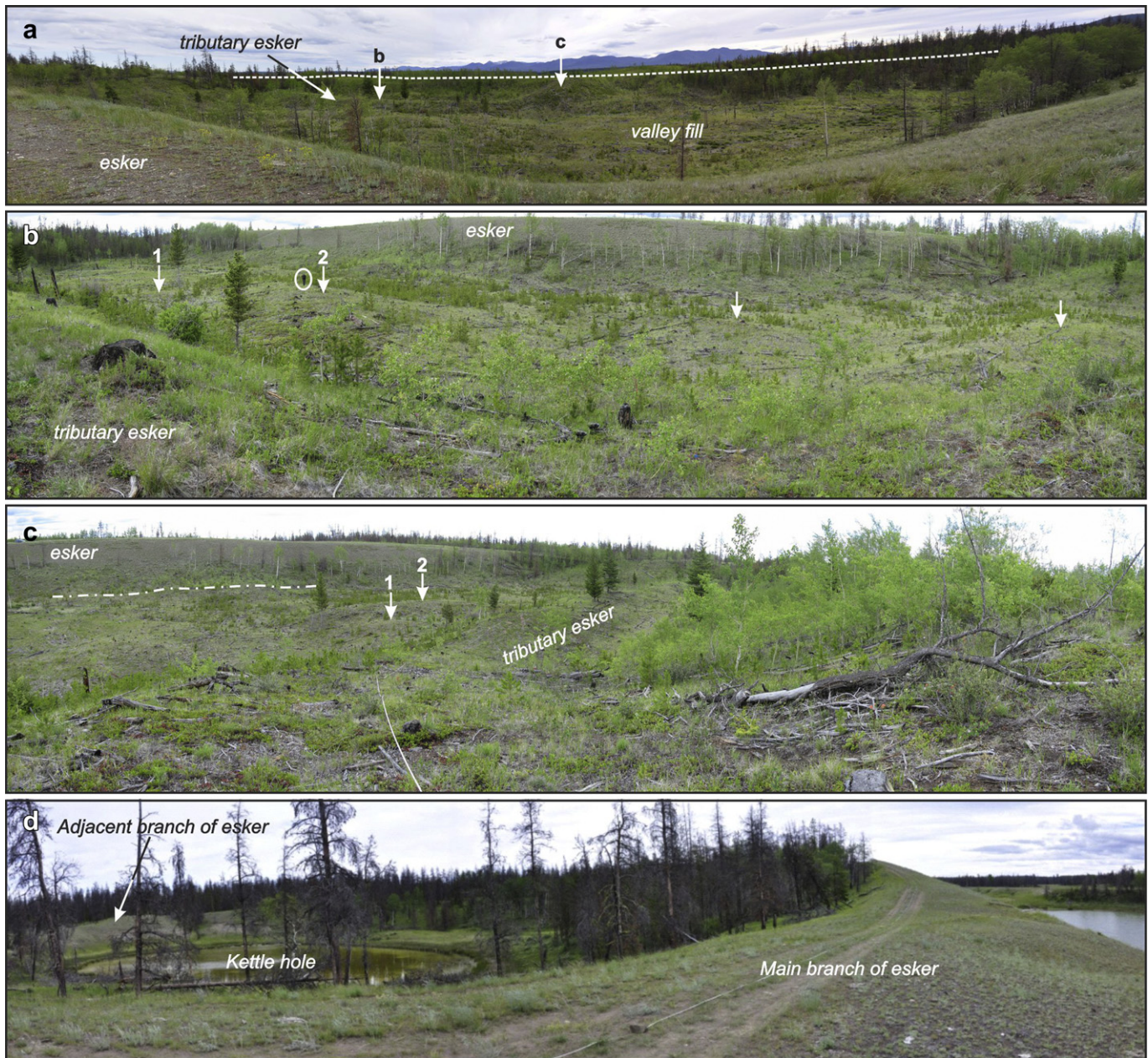
Fig. 3. Landforms within the Chasm meltwater corridor. a) A large main esker (esker) dominates the corridor fill. A small tributary esker drapes hummocks on the corridor floor. The meltwater corridor wall is highlighted by the dashed white line. Photograph taken from the main esker crest looking southwest. The arrows labelled "b" and "c" indicate the positions from which the photographs in b) and c) were taken, respectively. b) View of the corridor fill taken from the tributary esker and looking northeast. Some of the hummocks are arrowed, with those labelled 1 and 2 corresponding to the same hummocks labelled in c). Note person (∼1.8 m tall) for scale (circled). c) View of the eskers and corridor floor from the meltwater corridor wall, looking southeast. The labelled arrows indicate hummock crests on the corridor floor; the dot-dashed line highlights a linear ridge (slump) at the base of the main esker. d) The main esker at grid 2. The esker is anabranched here, with individual branches separated by kettle holes.

to the crestline of those hummocks and so dipping reflections appear flatter (cf. Russell et al., 2003).

Interpretation: Observations of the ground surface and limited exposures in the corridor fill (Fig. 6c, d) confirm that the high resistivity material (as shown in the ERT data, Fig. 5) corresponds to sand and coarse gravel (ranging from pebble-gravel to boulder-gravel; Fig. 6c,d). The lowest radar element (RE-B) is composed of sub-horizontal reflections that have characteristics consistent with plane beds identified in other GPR surveys (Heinz and Aigner, 2003; Burke et al., 2008, 2010). The tabular, sheet-like geometry of RE-B suggest it was likely deposited as broad gravel sheets indicative of high velocity (Heinz and Aigner, 2003; Rice et al., 2009), fluidal

flow (Russell et al., 2003). However, RE-B cannot be identified throughout the grids (Figs. 4 and 5), suggesting that gravel sheet deposition was discontinuous down and across flow, which is consistent with the characteristics of gravel sheets identified in Laurentide Ice Sheet tunnel channels (Russell et al., 2003).

Stratigrahically above RE-B at grid 1 are RE-C to RE-J that correspond to hummocks at the ground surface. These hummocks have erosional lower bounding surfaces. Internal dipping reflections have characteristics similar to dipping reflections identified in other GPR surveys (e.g., Fiore et al., 2002; Burke et al., 2008) and so are interpreted as foreset beds. The presence of foreset beds within these hummocks is consistent with the migration of large
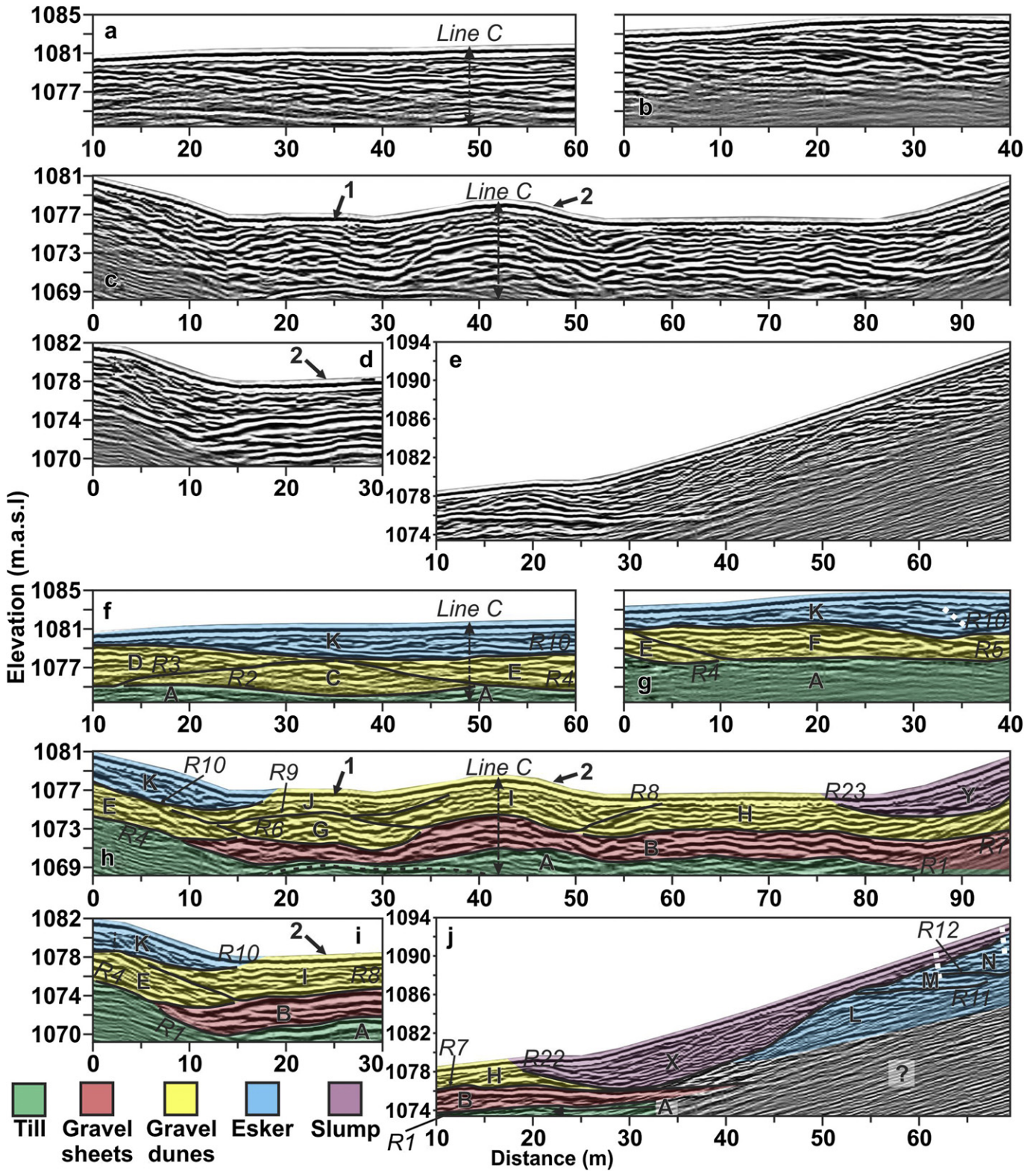
Fig. 4. GPR data collected over corridor fill at grid 1 (Fig. 1c). a) Line A1; b) line A2; c) line B; d) line C; e) line D. The locations where line C intersects line A1 and line B are shown by the labelled double arrows. The single arrows labelled 1 and 2 highlight the ground surface position of the same labelled hummocks in Fig. 3. Interpretation of f) line A1; g) line A2; h) line B; i) line C; j) line D. Radar bounding surfaces are highlighted by the bold lines and are labelled R1–R12 and R22–R23. These bounding surfaces define sixteen radar elements labelled A–N and X–Y. The locations where line C intersects line A1 and line B are shown by the labelled double arrows. The stippled line in c) highlights a diffraction (from a surface reflector) that has been distorted by topographic correction during data processing. White dashed lines mark offset reflections. The single arrows labelled 1 and 2 highlight the radar elements that correspond to the same labelled hummocks in Fig. 3. Colours correspond to stratigraphic element associations in legend and Table 1. (For interpretation of the references to colour in this figure legend, the reader is referred to the web version of this article.)
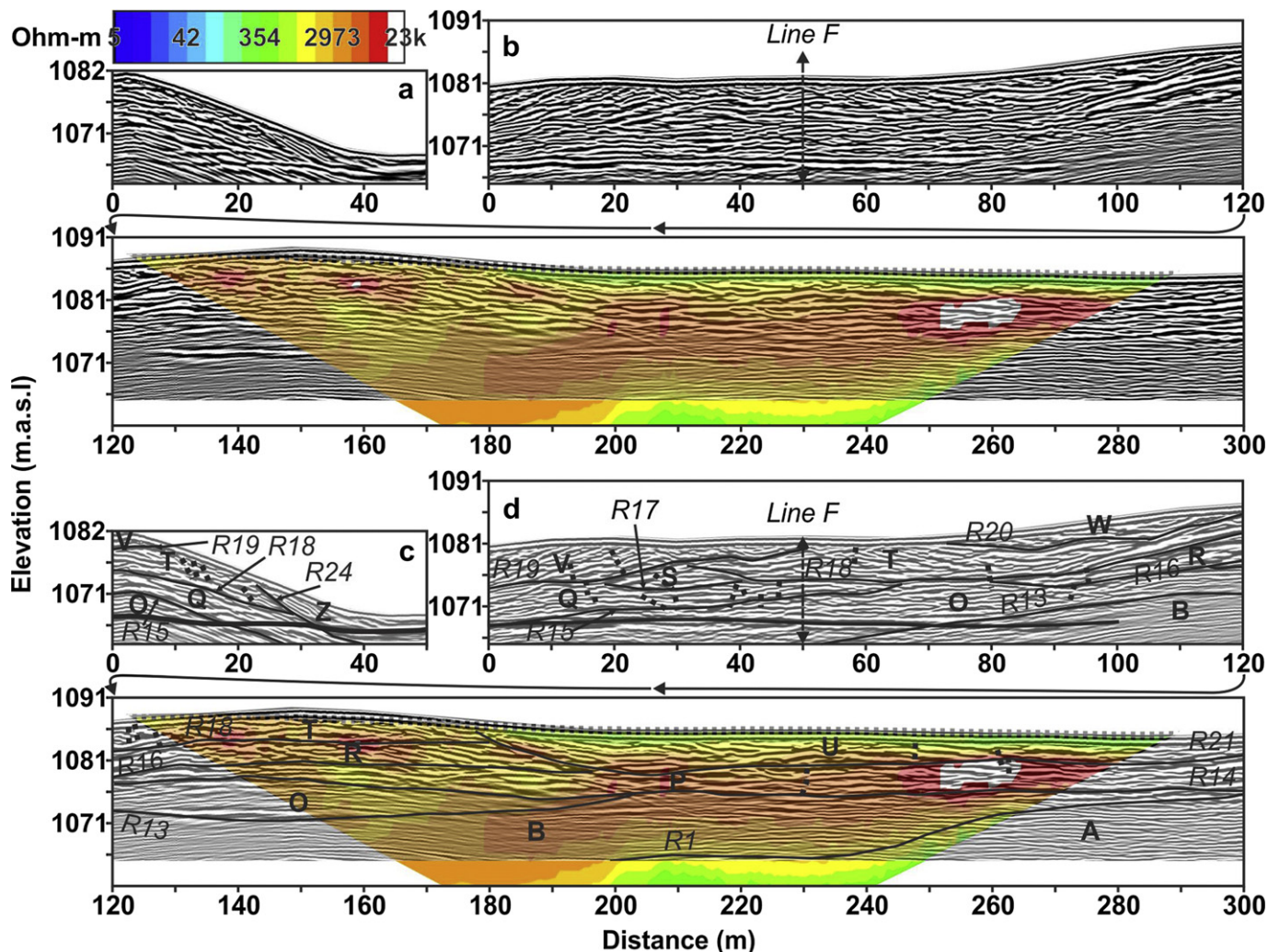
Fig. 5. GPR and ERT data collected at grid 2 (Fig. 1d). a) Line F; and b) line E. The location where line F intersects line E is shown by the labelled double arrow. Interpretation of c) line F; and d) line E. Radar bounding surfaces are highlighted by the bold lines and are labelled R1, R13–R21 and R24. These bounding surfaces define twelve radar elements labelled A–B, O–W and Z. The location where line F intersects line E is shown by the labelled double arrow. Dashed lines mark offset reflections. The ohm-m scale for the ERT data is at the top left of the Figure. Ohm-m values >13 000 (white) are the result of measuring air (high resistivity) along a narrow, steep segment of the main esker.
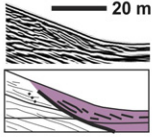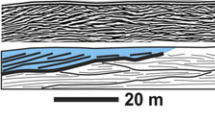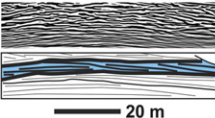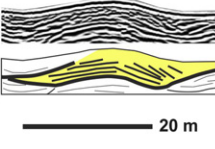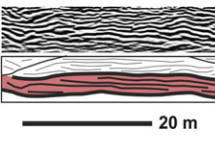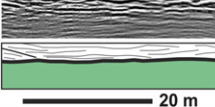
asymmetric gravel dunes (flow towards the southeast). Large, metre-scale gravel dunes are often identified in tunnel channel/valley fills and have usually been interpreted to indicate subglacial high-magnitude flow (Shaw and Gorrell, 1991; Pugin et al., 1999; Russell et al., 2003; Fisher et al., 2005). At grid 1 both dune morphology (Fig. 3a, b) and internal reflection geometry (Table 1 and Fig. 4) indicate they are 3-D forms. Based on the extent of RE-I, which can be directly linked to the surface expression of the bedform (2 in Fig. 3b, c), these gravel dunes are up to ∼4 m high, have stoss side, lee side and crestline lengths of ∼15 m, ∼10 m and ∼60 m respectively, and have wavelengths of ∼25 m. These dune dimensions are similar to those identified in Google earth© ∼18 km downflow within the Chasm corridor, a widening in the Green Lake corridor (Fig. 1b), and to metre-scale gravel hummocks in other meltwater corridor and tunnel channel/valley fills (cf. Gorrell and Shaw, 1991; Utting et al., 2009). If subaerial bedform wavelength and height to flow depth scaling relations can be applied to bedforms identified in the meltwater corridor (wavelength to depth ratio of 5:1 and dune height to flow depth ratio of 1:6 (Allen, 1984)), a flow depth of ∼5–20 m is estimated. Consequently, flow depth within the Chasm meltwater corridor would have been greater than meltwater corridor wall height (corridor wall height is ∼15 m at grid 1) along most of its length, suggesting that flow was corridor-

wide, bankfull, and partially contained by ice. As dune morphology (Fig. 2) and internal architecture (Figs. 4 and 5) appear intact there must have been little, if any, waning stage reworking. This, coupled with the lack of a fine sediment drape, point to a rapid flow-waning stage following dune deposition. Because both the gravel sheets and the gravel dunes are stratigraphically below the eskers (see § 4.2.3) and within the subglacially-eroded corridor walls, those radar elements must have been deposited subglacially.

4.2.3. Esker elements (RE-K to RE-W)

At grid 1, four radar elements (RE-K to RE-N) are imaged above the dunes and below R22 (blue, Fig. 4). RE-K to RE-N are lenticular elements composed of moderately continuous reflections that are either sub-parallel to the lower bounding surface (e.g., RE-K, Fig. 4a, f) or dip towards the esker flank (RE-L, Fig. 4e, j). No channel fill hummocks are identified at grid 2, but nine radar elements (RE-O to RE-W) are imaged above the gravel sheets (RE-B), and below R24 (Fig. 5). RE-O to RE-W have a high resistivity (∼1500–13,000 Ω-m, Fig. 5b, d), show significant complexity in line E (flow parallel, Fig. 5b, d), and RE-O, RE-Q, RE-T and RE-V extend across the full width of line F (flow perpendicular, Fig. 5a, c). RE-P, and RE-R to RE-T are stacked vertically (Fig. 5b, d) and composed of subhorizontal reflections that drape or onlap the lower bounding surface. RE-O,

Table 1
Summary of radar elements and meltwater corridor stratigraphy.

Stratigraphic Element Associations[a]	RE	RE Characteristics[b]	RE Interpretation
Post glacial elements	X - Z	• Concave-up and trough-like • Located on esker flanks • Initiate at offset reflections (faults) • Composed of discontinuous and chaotic reflections	Slump
Esker elements	O, Q, V	• Stacked in an upflow direction • Composed of relatively continuous upflow dipping reflections	Upglacier-stacked units of backset beds
	K-N, P, R-U, W	• Stacked with a tabular geometry • Composed of relatively continuous reflections, subparallel to the lower bounding surface	Vertically-stacked units of plane beds
Broad corridor fill elements	C-J	• Lenticular, convex-up, stacked hummocks • Composed of irregular reflections that may dip down-flow at hummock lee-side (where profile is near perpendicular to crest)	Gravel dunes
	B	• Broad with a sheet-like geometry • Composed of relatively continuous sub-horizontal reflections that drape or onlap the lower bounding surface	Gravel sheets
Corridor subtrate	A	• High-amplitude and irregular upper bounding surface • Largely reflection free • Rapid GPR signal attenuation	Till

[a]Refer to § 4.1 for further description and explanation.
[b]Example GPR data (above) and interpretation (below) for each RE type. Colour-coding corresponds to that used in Fig. 4.

RE-Q, RE-T and RE-V are stacked in an upflow direction (e.g., RE-Q against RE-O, Fig. 5d) and are composed of continuous reflections that are either subparallel to the lower bounding surface (e.g., RE-Q, Fig. 5d) or dip upflow (e.g., RE-V, Fig. 5d) at a high angle (∼ 14°). RE-U and RE-W have lenticular, concave-up geometries (<7 m thick), lower bounding surfaces that truncate deeper reflections, and are composed of subparallel reflections that drape or onlap the lower bounding surface (e.g., RE-U, Fig. 5d). Offset reflections are most common in flow-perpendicular lines (e.g., Lines D (Fig. 4, j) and F (Fig. 5, d)), but overall, these reflection offsets do not result in significant distortion of primary reflection geometry.

Interpretation: At grid 1, the geometry and position of RE-K corresponds to that of a small tributary esker (Fig. 3a–c), whereas RE-L to RE-N correspond to the main esker, which is flat topped here (Fig. 3a–c). At grid 2, RE-O to RE-W record the main esker that has a round-crested morphology (Fig. 3d). The high resistivity of the esker radar elements at grid 2 (though slightly lower than that of the broad gravel sheets: RE-B, Fig. 6), suggests a composition of sand and gravel, which is confirmed by the dominance of sand and pebble gravel in outcrop at grid 1 (Fig. 6a) and at the landform surface at grid 2 (Fig. 6b). Flow perpendicular lines suggest that these radar elements were deposited within an ice tunnel at least 25 m in width, though, based on their geometry, they probably extend beyond the limits of the GPR lines and so the ice tunnel was

likely wider. Subhorizontal reflections are consistent with the deposition of plane beds (composed of sand and pebble gravel, Fig. 6a, b) by high velocity flow. These plane bed units conform to the geometry of deeper radar elements and were likely deposited within a relatively constricted ice tunnel (cf. Burke et al., 2008, 2010). However, upflow dipping reflections are most likely backset beds because their reflection characteristics and angle of dip are similar to those reported for other eskers (e.g., Fiore et al., 2002; Burke et al., 2008, 2010), and they do not dip at angles parallel to their lower bounding surfaces. Backset beds in eskers are thought to indicate the presence of a hydraulic jump associated with an abrupt ice tunnel widening (e.g., Brennand, 1994; Fiore et al., 2002).

In flow parallel lines, the orientation and stacking of radar elements, coupled with internal reflection geometry, can be used to infer depositional direction: vertically-stacked radar elements indicate vertical accretion of plane beds; upglacier-stacked elements that are primarily composed of backset beds record headward enlargement of the ice tunnel (cf., Brennand, 1994; Brennand and Shaw, 1996; Burke et al., 2008, 2010); and lenticular, concave-up radar elements that have erosional lower bounding surfaces are consistent with scour-and-fill (e.g., Heinz and Aigner, 2003), perhaps recording a reduction in flow depth as the ice tunnel filled with sediment. The presence of (probably) ridge-wide vertically-stacked, upflow-stacked, and scour-and-fill radar
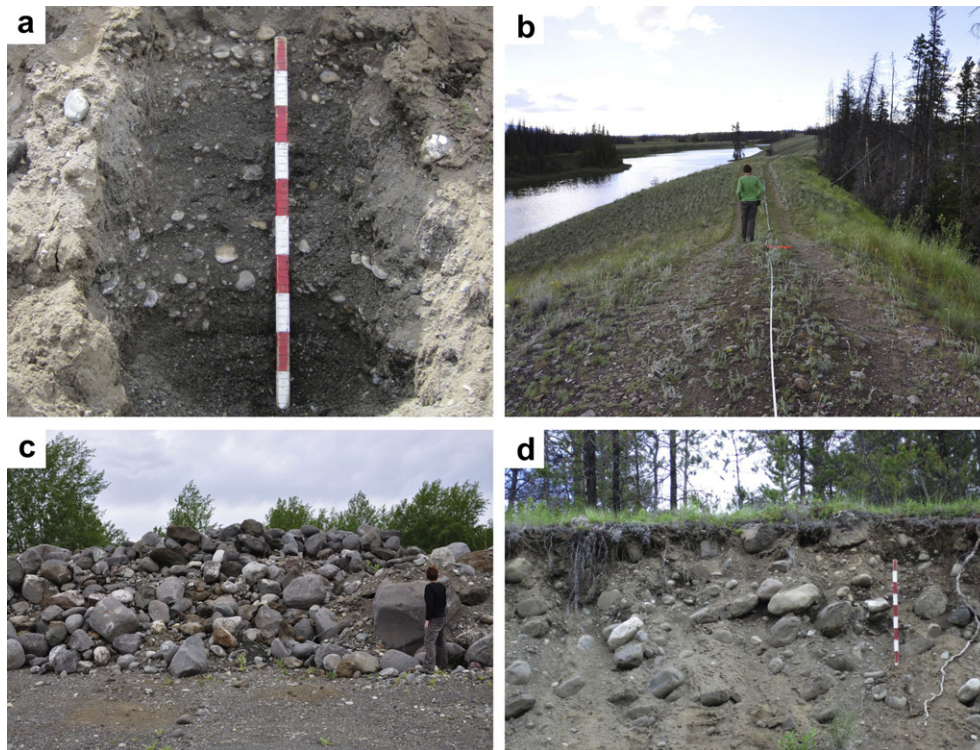
Fig. 6. Material observed within meltwater corridor fill. a) Sediment section within the main esker at grid 1, showing the landform is dominated by sand to pebble-gravel. Divisions along the 1 m rid are at 0.1 m intervals. b) Sand and pebble- to cobble-gravel at the surface of the main esker at grid 2. Note person for scale. c) Boulder-gravel Piled up within a gravel pit at the downglacier end of the Chasm meltwater corridor (see Fig. 1b for location). Note the person for scale. d) Imbricated boulder-gravel at the downglacier end of the Green Lake meltwater corridor (see Fig. 1b for location). Divisions along the 1 m rod are at 0.1 m intervals. Refer to Fig. 1b for photograph locations.

elements within a 300 m long round-crested section of esker is consistent with the architecture of esker macroforms that are thought to indicate rapid, high-energy deposition in a subglacial ice tunnel (Brennand, 1994; Burke et al., 2010).

The presence of offset reflections (faults, dashed lines, Figs. 4 and 5) predominantly towards the flanks of the eskers probably indicate sediments were deposited in contact with ice (Burke et al., 2008; Woodward et al., 2008; Burke et al., 2010; Burke et al., submitted for publication). However, the limited extent of post-depositional reworking and distortion of primary reflection geometry within the esker (cf. Burke et al., submitted for publication) suggests that they were not deposited englacially or supraglacially (Brennand, 1994, 2000).

Although the internal architecture and round-crested morphology of the main esker at grid 2 (Fig. 3d) is consistent with subglacial deposition (Brennand, 1994, 2000), the flat-topped morphology of the main esker at grid 1 (Fig. 3a–c) is more consistent with deposition within a subaerial, unroofed, ice-walled canyon (Russell et al., 2001; Burke et al., 2008). The presence of a subaerial ice-walled canyon (grid 1) upflow of a subglacial ice tunnel (grid 2) would require the ice to be thin enough to allow local conduit unroofing following continuous subglacial ice-tunnel flow. This inference is supported by the undisturbed internal architecture of the underlying corridor fill, which suggests that sediment deformation expected from thick ice-bed recoupling and sliding did not take place (Brennand, 1994).

4.2.4. Post glacial elements (RE-X to RE-Z)

The stratigraphically highest radar elements are RE-X to RE-Z, the lower bounding surfaces of which truncate the radar elements within the main esker at grids 1 and 2 (Figs. 4 and 5). The heads of these radar elements correspond to offset reflections (faults) within the esker (e.g., at ~61 and 68 m of line D, Fig. 4j) and they are

composed of chaotic reflections. At the base of the esker flank, RE-X to RE-Z correspond to linear blocks of esker material (Fig. 3c).

Interpretation: RE-X to RE-Z are interpreted as slumped esker material formed due to removal of ice support because: 1) they are associated with faults within the esker flanks; 2) they are composed of chaotic, irregular reflections that indicate poorly sorted or disturbed material; and 3) they form parallel linear ridges of esker material at the base of the esker flank.

5. Evolution of the subglacial hydrologic system

5.1. Single event or multiple event formation?

The meltwater corridors on the southern Fraser Plateau are deeply eroded into bedrock at their downflow ends and shallowly incised into till (and/or bedrock) upflow. The large bedrock cataracts present at the corridor termini were probably generated over multiple glaciations (Fisher et al., 2005; Plouffe et al., 2011), acting as low pressure sinks that focused seasonal subglacial water flow. The presence of these cataracts raises the possibility that the meltwater corridors upglacier were also generated over multiple events. However, upglacier from the cataracts the corridors are mainly incised into till. Because this till was most likely deposited during the last glacial period (cf. Huntley and Broster, 1994, 1996; Lian and Hicock, 2000, 2001; Plouffe et al., 2011) it is also likely the corridors were eroded by an event(s) following LGM. Although we cannot rule corridor erosion over multiple events, we suggest they were formed during a single event because: 1) meltwater corridor fill includes extensive gravel sheets, large gravel dunes and eskers composed of ridge-wide macroforms; testament to high-magnitude deposition (cf. Burke et al., 2010) and, by extension, erosion of the corridors; 2) dune scale suggests flow depth was greater than the height of the corridor walls during their deposition indicating flow was probably

corridor wide; 3) the broad corridor fill has not been reworked following deposition nor is it buried by waning stage fines. This is consistent with collapse of the broad flow that deposited the dunes into an esker-forming ice tunnel on the waning stage, but inconsistent with corridor-wide water flow through the corridor following deposition of this fill; 4) the walls of the discontinuous trough components of the meltwater corridors are underdeveloped (unless wall discontinuity is associated with variation in till thickness; this is hard to test because till thickness map resolution is too low), suggesting broad water discharge (inferred from dune scale to flow depth relationships) through the corridors was short lived. Had the meltwater corridors been re-occupied by repeated high-magnitude events, their walls would presumably be better developed. Consequently, we interpret the discontinuous trough components of the meltwater corridors to have operated as efficient canals (tunnel channels); i.e., channels incised down into subglacial sediment and up into the overlying ice (cf. Walder and Fowler, 1994; Ng, 2000).

5.2. Water source

If the meltwater corridors had been developed from basally-derived meltwater they would likely form a branched network (Boulton and Hindmarsh, 1987; Fountain and Walder, 1998), yet the corridors are single thread canals that begin abruptly. This suggests waters originated from a point source (Lesemann et al., 2010) and we attribute their formation to either supraglacial or subglacial lake drainage because they are large and filled with sediments recording a high-magnitude event. Lake sediments are identified in an area immediately upflow of the meltwater corridors (Fig. 7). Immediately downglacier from, and surrounding the southern margin of these lake sediments, linear ridges (ribbed terrain) of sediment (normal to ice flow direction) are identified (Fig. 7b). The coincidence of the lake sediments with the heads of the meltwater corridors suggest the lake in which they were deposited may have been a water source for corridor formation and therefore subglacial. Furthermore, the presence of coincidental ridges (ribbed terrain) suggests glaciotectonic bed deformation (cf. Stokes et al., 2007, 2008). If these ridges are associated with bed deformation (unfortunately, there is no ground-based data to verify this) this may have been induced by the presence of a subglacial lake that lubricated the overlying ice; compressive stresses in the bed induced by slower grounded ice flow downflow of the subglacial lake likely resulted in the production of glacitectonic ridged terrain. Modelling of the hydraulic potential (refer to Supplementary material for details) suggests subglacial meltwater ponding could have occurred at the heads of the meltwater corridors and that this subglacial lake would have had an area of $\sim$132 km^2 (Fig. 7) and stored $\sim$1.5 km^3 of water. If the canals were contemporaneously filled with water along their length they would have accommodated $\sim$0.3 km^3 (Chasm canal) and $\sim$0.6 km^3 (Green Lake canal) of water.[1] Assuming all of the water stored within the modelled subglacial lake drained, it would have contained sufficient water to maintain bankfull flow through the canals for some time, even if they were generated synchronously by the same lake drainage. On the other hand, if supraglacial lakes were the water source, assuming a lake depth of 10 m (similar to depths reported from the GrIS (Krawczynski et al., 2009)), the minimum supraglacial lake diameter would be $\sim$5.5 km and $\sim$7.5 km^2 for the Chasm and Green

Lake corridors, respectively. However, the actual lake diameters must have been significantly larger in order for high-magnitude flows to persist for sufficiently long to accomplish the geomorphic work observed. Indeed, supraglacial lakes on the GrIS often range in diameter from $\sim$1 to 12 km (McMillan et al., 2007; Krawczynski et al., 2009). It is unclear whether or not the Chasm and Green Lake meltwater corridors were generated during the same or separate events. However, drainage of a subglacial lake would likely result in collapse of the overlying ice to form an ice surface depression in which a supraglacial lake could form. Thus, if one of the corridors was indeed generated by subglacial lake drainage, it is possible the other could have formed later due to drainage of a supraglacial lake that formed in the ice surface depression induced by subglacial lake drawdown.

5.3. Evolution of the glacial hydrological system

A rapid rise in equilibrium line altitude is thought to have resulted in stagnation and downwasting of the CIS over BC's southern interior plateaus (Fulton, 1991; Clague and James, 2002). During this time significant supraglacial meltwater would likely have accessed the bed through crevasses and moulins. However, local depressions on the downwasting ice sheet surface and ice sheet bed would have trapped water to form supraglacial (Scenario A, Fig. 8) and/or subglacial lakes (Scenario B, Fig. 8), respectively.

5.3.1. Scenario A: supraglacial lake drainage (stages A1–A3)
Because the ice was stagnant at the time of corridor development (as inferred from the lack of large recessional moraines, cf. Fulton, 1991), the potential for extensional crevasse formation was low, and so englacial routing of supraglacial lake water to the bed must have been via pre-existing structures, remnant of earlier, more active ice conditions (cf. Plouffe et al., 2011). Incipient crevasses beneath supraglacial lakes could have allowed fracture propagation along the pre-existing weaknesses (stage A1, Fig. 8), with the presence of the lake providing sufficient water for fracture penetration to the bed (Alley et al., 2005; Das et al., 2008; Krawczynski et al., 2009). At the point of water input to the bed a well-established drainage network was absent and so floodwaters slowly propagated as a broad floodwave (inefficient drainage) (stage A2, Fig. 8).

5.3.2. Scenario B: subglacial lake drainage (stages B1–B2)
The modelled subglacial lake existed within a depression at the ice sheet bed (Fig. 7). Subglacial lake growth would have continued until the critical point for drainage was reached, probably via ice-dam flotation (Tweed and Russell, 1999). Immediately downglacier from the putative subglacial lake the Chasm and Green Lake meltwater corridors are defined by broad (up to 2.5 km wide) zones of scabbed topography (Fig. 2 a, b). This scabbed topography records flow of water over broad zones (stage B1, Fig. 8), suggesting that any pre-existing subglacial drainage network could not respond rapidly enough to the sudden influx of water. Instead, the initial floodwater was discharged through a broad floodwave (inefficient drainage) (stage B1, Fig. 8).

Given the coincidence of lake sediments with the meltwater corridors and surrounding ribbed terrain, we cannot rule out the possibility of subglacial lake drainage. However, although our modelling suggests a subglacial lake could have existed here, we favour a supraglacial water source because: 1) the model parameters required to pond water in a subglacial lake in Dog Creek basin, including the topography of the ice sheet bed at the time of lake drainage, ice thickness, and ice surface slope, are poorly constrained; and 2) the existence of a subglacial lake requires strict

---

[1] Water volumes were calculated based on an assumption that the canal was a uniform cuboid, using median measurements of width and wall height.

[2] Supraglacial lake diameter estimates are a minimum based on the assumptions that the lakes were cubes and that they contained a water volume equivalent to that required to achieve a single bankfull flow through the corridors (see footnote[1]).
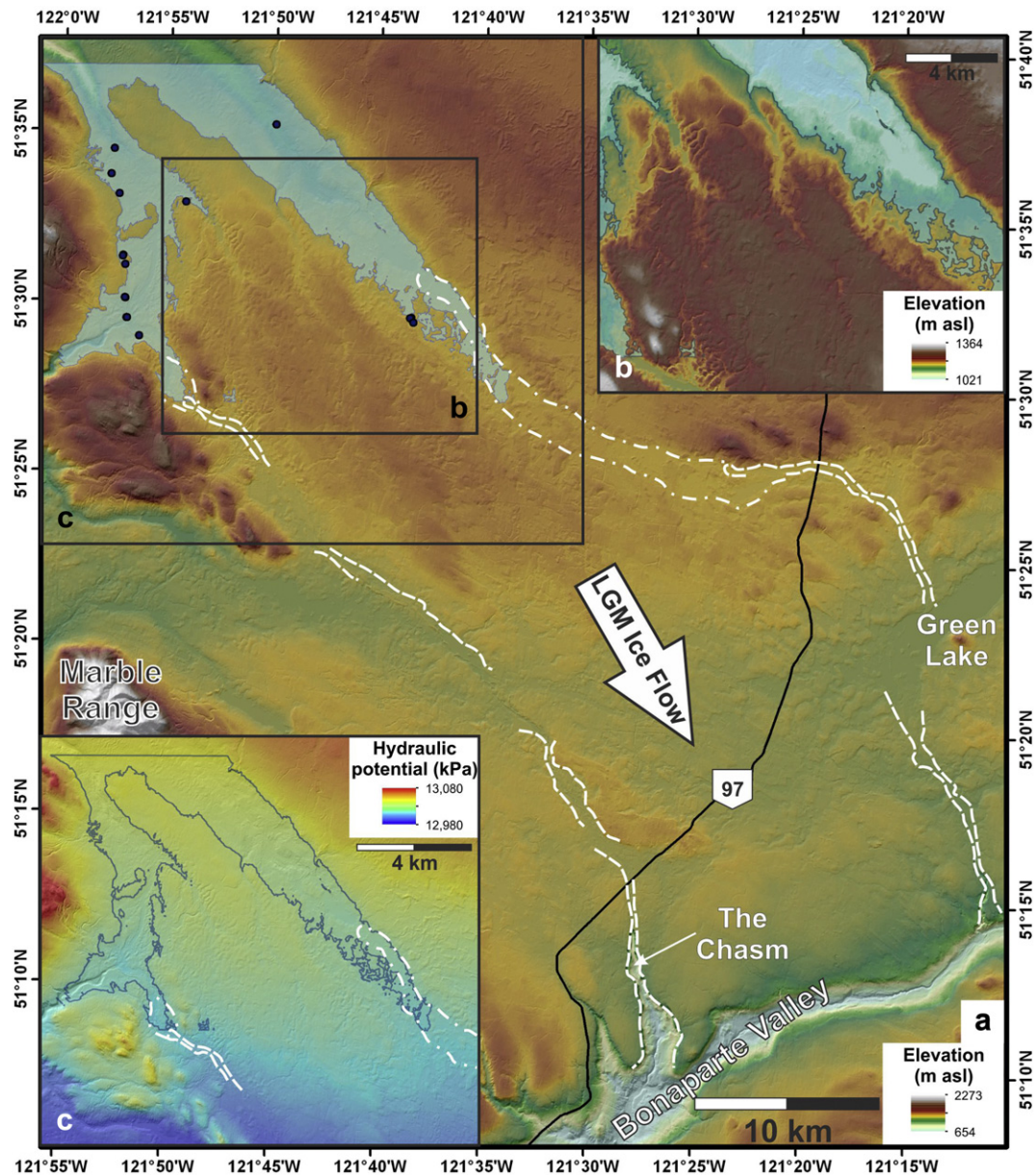
Fig. 7. a) A hillshaded elevation model of the southern Fraser Plateau (Geobase®). The Chasm and Green Lake meltwater corridors are shown: the dashed lines are the discontinuous troughs, whereas the dot-dashed lines highlight the extent of scabbed terrain. The dots show the distribution of lake sediment sections in Dog Creek basin; the semi-transparent blue polygon is a modelled subglacial lake surface projected over an elevation model. The lake was modelled with an ice surface slope of 0.015° (azimuth of 170.78°) and the western valleys filled (to simulate sediment infill) up to 1126 m asl. The labelled white arrow indicates ice flow direction at last glacial maximum (LGM). The labelled boxes highlight the location of insets b) and c). b). Zoomed view of ribbed terrain (northeast−southwest orientated linear ridges) surrounding the downglacier end of the subglacial lake (semi-transparent blue polygon). c) Hydraulic potential (kPa) calculated for the subglacial lake (blue outline) bed and surrounding area. Meltwater corridors are shown by dot-dashed (scabbed terrain) and dashed (discontinuous troughs) lines. Details of the subglacial lake modelling and hydraulic potential calculation are presented in the Supplementary content. (For interpretation of the references to colour in this figure legend, the reader is referred to the web version of this article.)

antecedent glaciological and topographical conditions that are probably unreasonable (refer to Supplementary content).

5.3.3. Canalization and corridor fill deposition (stages C–G)

Following ice-dammed lake drainage initiation, any pre-existing subglacial drainage network could not respond rapidly enough to the sudden influx of water, so initial floodwave advance was gradual, inefficient, and over a relatively broad area (stage A2 and B1, Fig. 8). We suggest that the minimum extents of these broad floodwaves correspond to that of the scabbed topography immediately upflow of the Chasm and Green Lake canals (Fig. 2a, b). Scabbed erosion was limited to the upglacier parts of the meltwater

corridors, and within 3–24 km of the water source floodwaters were entirely focussed into canals <2.5 km wide because there is no scabbed terrain here. The absence of broad scabbed erosion along the full length of the meltwater corridors (i.e. alongside the discontinuous trough components) argues against collapse of broad inefficient flow into smaller efficient canals as the flood developed. Instead broad flow is abruptly focussed into the canal heads (erosional remnants are roughly aligned to the canal heads), suggesting that efficient ice tunnels must have pre-existed at downglacier sections of the meltwater corridors. Seasonally beneath the GrIS, headward development of efficient channel networks (McMillan et al., 2007; Sole et al., 2011) can result in
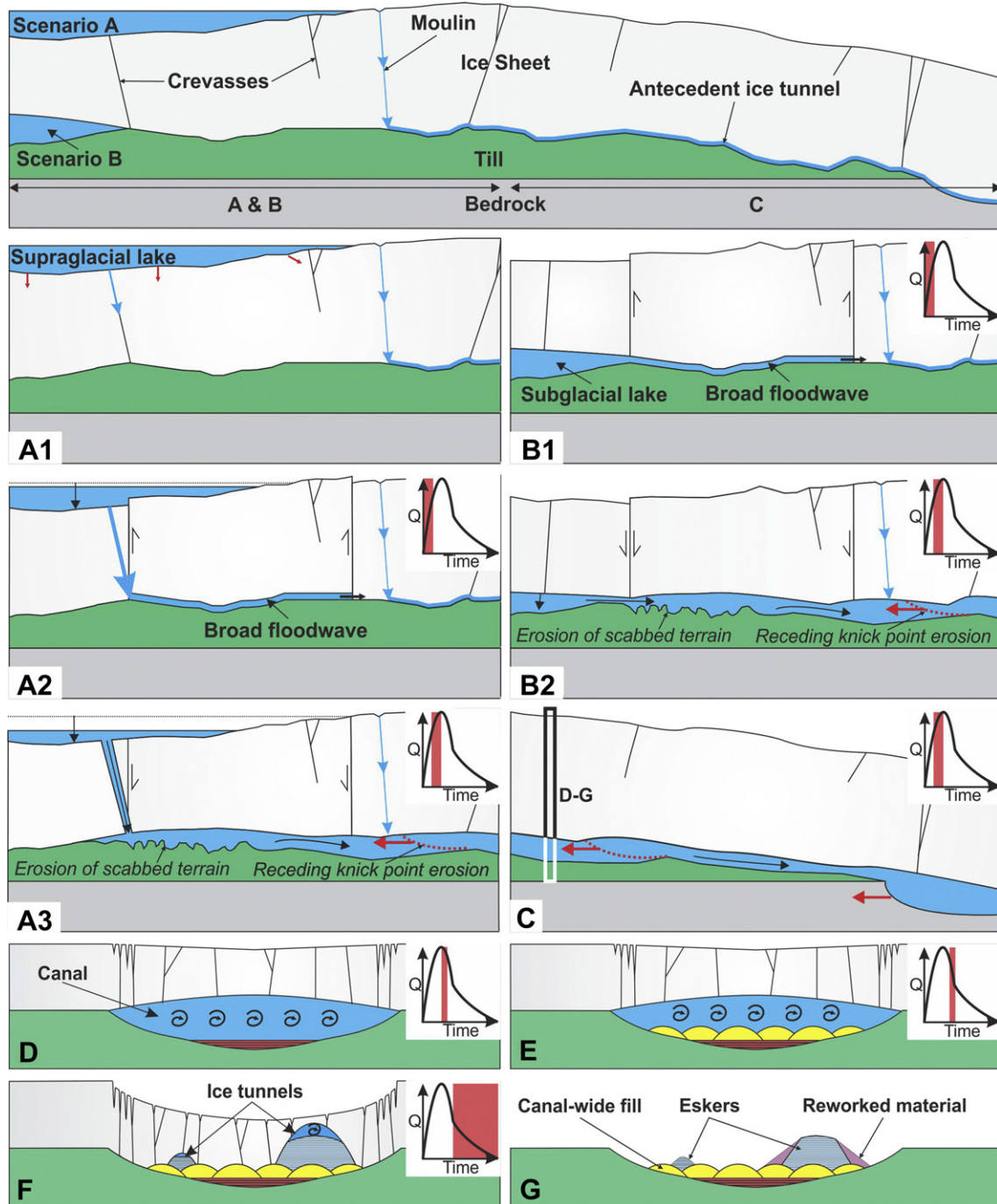
Fig. 8. Cartoon depicting meltwater corridor evolution on the southern Fraser Plateau during supraglacial (scenario A) or subglacial (scenario B) lake drainage (not to scale). A1–3 and B1–2 are a view of the upglacier part of the system; C is the downglacier component. A1) Supraglacial lake formation resulted in hydrofracture propagation along an incipient crevasse. A2) Upon reaching the bed, any pre-existing drainage network could not respond rapidly enough to the sudden input of water and so water was discharged through a broad floodwave (inefficient drainage). A3) Intersection of the broad floodwave with an efficient antecedent ice tunnel downglacier resulted in erosion of broad scabbed terrain upglacier. B1) Subglacial lake enlargement would have eventually reached the critical point for drainage. Because any pre-existing drainage network could not respond to the sudden influx of water, it spread to form a broad floodwave (inefficient drainage) downglacier. B2) Intersection of the broad floodwave with an antecedent ice tunnel downglacier resulted in erosion of broad scabbed terrain upglacier. C) Rapid enlargement of an antecedent Ice tunnel restricted erosion width downflow. Channel enlargement included receding knickpoint erosion of the bed. Following development of efficient canal flow, gravel sheets (D), dunes (E), and eskers (F) were deposited. Corridor fill colouring corresponds to that in Table 1 and Fig. 5. Inferred hydrograph stage is indicated by red shading on a hydrograph (stages A–F). G) Ice sheet decay removed lateral support from esker sediment and resulted in esker flank collapse. Stages A–C are depicted in flow parallel perspective and stages D–G are in flow transverse perspective. See § 5.3 for a full explanation. (For interpretation of the references to colour in this figure legend, the reader is referred to the web version of this article.)

efficient drainage systems that extend for up to 48 km from the ice sheet margin (e.g., Sole et al., 2011). On the Fraser Plateau the canals extend for up to 40 km before scabbed terrain can be identified. We envisage the presence of antecedent, seasonal ice tunnels that were

developed due to increasing amounts of supraglacial meltwater input to the bed (via moulins) throughout the earlier melt season. Upglacier from these antecedent channels, any pre-existing drainage networks were inefficient and so floodwaters were

discharged as a slowly propagating broad floodwave (stage A2 and B1, Fig. 8). Downglacier, the existence of efficient subglacial ice tunnels allowed waters to be quickly evacuated from the bed once the broad floodwave intersected the pre-existing ice tunnels. Focussing of the broad floodwave into the ice tunnels was like "pulling the plug" on this slowly propagating floodwave, increasing the flow velocity of water within the floodwave as it was focussed into the ice tunnel, eroding the scabbed terrain (stage A3 and B2, Fig. 8). However, the antecedent ice tunnels would not have been of sufficient geometry to evacuate all floodwater from the bed and so must have been enlarged rapidly through incision into the over-lying ice and underlying bed to form efficient canals that could accommodate the sudden increase in discharge. Had the ice tunnel not developed rapidly, water would have been forced to spread over a broader area, evidence for which is lacking. Indeed, the walls of the canals are discontinuous suggesting that canal-wide flow was short lived and partially ice-walled. Had the pre-existing drainage network been of an equivalent scale to that invoked by the canal geometries, it follows that the canal walls would be well-developed due to persistent meltwater flow during the preceding melt season(s). Furthermore, the presence of plunge pools and the horseshoe-shaped planform of both canal heads (Fig. 2a, b) indicate that subglacial canal development involved receding knickpoint erosion of recessional cataracts (stage C, Fig. 8), echoing headward recession of Dry Falls during the Missoula floods (Bretz, 1932) and evidence used to suggest high-magnitude tunnel channel devel-opment elsewhere (e.g., Wingfield, 1990).

The development of efficient canals would have facilitated rapid lake drawdown and the flood(s) would have risen to peak discharge quickly. The deepest deposits within the Chasm canal fill (gravel sheets) indicate deposition from high velocity flow across much of the canal width, which may have facilitated ice surface collapse and longitudinal crevassing along the flow path (Sundal et al., 2011; stage D, Fig. 8). Decreasing flow velocities resulted in deposition of large-scale asymmetric gravel dunes (stage E, Fig. 8). However, the underdeveloped canal walls (assuming this is not associated with variation in till thickness) suggest that bankfull flow was short lived, and the lack of dune reworking and burial by fine sediments point to a rapid flow waning that was quickly focused into a narrower ice tunnel, preventing reworking and burial of the canal-wide fill (stage F, Fig. 8). A flood origin for esker sedimentation is supported by esker composition (sand, gravel, a lack of fines), and the presence of ridge-wide macroforms (cf. Burke et al., 2010). Such collapse of broader flows into esker forming ice tunnels has been documented from contemporary jökulhlaups (Burke et al., 2008) and suggested for tunnel channel–esker associations elsewhere (Shaw, 1983). Rapid collapse of the canal-wide flow was likely facilitated by structural weaknesses in the ice (Burke et al., 2009), as demonstrated by the presence of kettle holes between esker branches (Fig. 3d). At LGM, ice on the interior plateaus was only up to ~600 m thick (Huntley and Broster, 1994). The lack of corridor fill reworking suggests there was no major drainage through the corridors after their formation. Thus, the event(s) that formed and filled them probably took place during the final stages of the CIS here at which time the ice must have been very thin. Although difficult to directly corre-late, ice-marginal meltwater channels on the lower slopes of the Marble Range indicate ice was ~100–300 m thick over the meltwater corridors at the time of ice-marginal meltwater channel formation. As the ice was likely thin during lake drainage, ice tunnel closure due to glaciostatic pressure would have been low, allowing a prolonged waning stage (Roberts, 2005) and complex esker deposition (stage F, Fig. 8). Following removal of ice support the esker flanks collapsed through both normal faulting and slumping (stage G, Fig. 8).

6. Conclusions and wider implications

Relatively low sinuosity meltwater corridors that dissect the southern Fraser Plateau in the interior of BC are shown to have formed subglacially as a broad floodwave was focussed into effi-cient canals. Although these canals are directly related to down-flow erosion of a large bedrock cataract, presumably over multiple glaciations, geophysical data reveal that the canals upflow are mainly eroded into till and so were likely generated during the last glaciation. This contrasts with the development of buried tunnel valleys in Europe over multiple glaciations (e.g., Piotrowski, 1994; Jørgensen and Sandersen, 2008). Fill within the Chasm and Green Lake canals indicate a relatively simple event sequence, consistent with high-magnitude flow and bankfull conditions due to ice-dammed lake drainage, as suggested for tunnel channels formed beneath the LIS (e.g., Shaw and Gorrell, 1991; Brennand and Shaw, 1994; Sjogren et al., 2002), and for large channels observed in Antarctica (Denton and Sugden, 2005; Wingham et al., 2006; Jordan et al., 2010). Our data implicate canal formation due to synchronous erosion and then deposition along the length of the individual canals, but also includes elements of headward devel-opment through receding knickpoint and plunge pool erosion. Consequently, our event sequence suggests that during canal (tunnel channel) formation, some erosional elements that were previously inferred to suggest time-transgressive development (Wingfield, 1990), may in fact be generated during synchronous formation. Thus, the presence of these elements alone cannot be used to infer time-transgressive tunnel channel development.

Our event sequence gives insight into the development of the subglacial hydrological system beneath a rapidly decaying ice sheet. At the AIS and land-terminating sections of the GrIS, ice velocity variations can be controlled by ice-dammed lake drainage (e.g., McMillan et al., 2007; Stearns et al., 2008; Sole et al., 2011). Although positive relations between transient subglacial meltwater flow and ice motion at both the AIS and GrIS have been proposed as mecha-nisms for facilitating significant mass loss from the polar ice sheets (Bell, 2008), such velocity increases require the presence of an inefficient and distributed drainage system (McMillan et al., 2007). Efficient drainage systems moderate the lubricating effect of water on ice velocity (Bartholemew et al., 2011; Sundal et al., 2011). Our data from the Fraser Plateau reveal that although ice-dammed lakes initially drained via a broad and inefficient floodwave upglacier, the downglacier presence of antecedent seasonal ice tunnels allowed rapid development of efficient canals during the final stages of the thin (Huntley and Broster, 1994) and stagnating (Fulton, 1991) CIS. The presence of these long seasonal ice tunnels implicates a large supraglacial meltwater supply. Because conduit closure rates are presumably limited beneath thin ice, floodwaters can quickly enlarge pre-existing drainage networks into efficient canals that rapidly evacuate floodwater, reducing the impact of ice-dammed lake drainage on ice velocity. Although it is difficult to propose direct analogies between the CIS and AIS, our data may aid future predictions of the role of ice-dammed lake drainage on subglacial hydrological system development beneath a thinning GrIS. In the short term climate warming may increase the influence of ice-dammed lake drainage on ice-bed velocities of land-terminating sections of the GrIS. However, our data suggest that once these sections have thinned below some threshold ice thickness (reducing conduit closure rates sufficiently) and there is sufficient meltwater reaching the bed to allow extensive efficient drainage networks to develop, the importance of ice-dammed lake drainage on ice dynamics may reduce. Given the potential importance of ice-dammed lake drainage on the dynamics of contemporary ice masses, further assessment of the role of ice-dammed lake drainage on ice acceleration and mass balance of former ice sheets is needed.

Identification of ice-dammed lake drainage signatures on the southern Fraser Plateau reveal a relatively simple event sequence that may aid better assessment of the influence of ice-dammed lake drainage on palaeo-ice sheets. Because former ice sheet beds are relatively accessible, detailed investigation of meltwater landforms can improve our understanding of subglacial hydrologic system evolution beneath ice sheets of varied glaciological conditions.

Acknowledgements

Appendix A. Supplementary data

Supplementary data associated with this article can be found, in the online version, at http://dx.doi.org/10.1016/j.quascirev.2012.07.005.

References

Allen, J.R.L., 1984. Sedimentary Structures Their Character and Physical Basis. Elsevier, New York.

Alley, R.B., Dupont, T.K., Parizek, B.R., Anandakrishnan, S., 2005. Access of surface meltwater to beds of sub-freezing glaciers: preliminary insights. Annals of Glaciology 40, 8–14.

Andrews, G.D.M., Plouffe, A., Ferbey, T., Russell, J.K., Brown, S.R., Anderson, R.G., 2011. The thickness of Beogene and Quaternary cover across the central interior plateau, British Columbia: analysis of water-well drill records and implications for mineral exploration potential. Canadian Journal of Earth Science 48, 1–14.

Andrews, G.D.M., Russell, K., Dohaney, J., Brown, S.R., Caven, S., Anderson, R.G., 2009. The Case for Prolonged Neogene Regional Uplift in BC's Interior Plateau. 105th Cordilleran Section Meeting. Geological Society of America, University of British Columbia, Okanagan, BC. Paper No. 11–8.

Arcone, S.A., Lawson, D.E., Delaney, A.J., 1995. Short-pulse radar wavelet recovery and resolution of dielectric contrasts within englacial and basal ice of Matanuska Glacier, Alaska, U.S.A. Journal of Glaciology 41 (137), 68–86.

Bartholomew, I.D., Nienow, P., Mair, D., Hubbard, A., King, M., Sole, A., 2010. Seasonal evolution of subglacial drainage and acceleration in a Greenland outlet glacier. Nature Geoscience 3, 408–411.

Bartholomew, I.D., Nienow, P., Sole, A., Mair, D., Cowton, T., King, M.A., Palmer, S., 2011. Seasonal variations in Greenland Ice Sheet motion: inland extent and behaviour at higher elevations. Earth and Planetary Science Letters 307, 271–278.

Bell, R.E., 2008. The role of subglacial water in ice sheet mass balance. Nature Geoscience 1, 297–304.

Beres, M., Haeni, F.P., 1991. Application of ground-penetrating radar methods in hydrogeologic studies. Ground Water 29 (3), 375–386.

Booth, D.B., 1994. Glaciofluvial infilling and scour of the Puget Lowland, Washington, during ice-sheet glaciation. Geology 22, 695–698.

Booth, D.B., Hallet, B., 1993. Channel networks carved by subglacial water: observations and reconstruction in the Puget lowland of Washington. Geological Society of America Bulletin 105, 671–683.

Booth, D.B., Troost, K.G., Clague, J.J., Waitt, R.B., 2003. The Cordilleran Ice Sheet. Developments in Quaternary Science 1, 17–43.

Boulton, G.S., Hindmarsh, R.C.A., 1987. Sediment deformation beneath glaciers: rheology and sedimentological consequences. Journal of Geophysical Research 92, 9059–9082.

Box, J.E., Ski, K., 2007. Remote sounding of Greenland supraglacial melt lakes: implications for subglacial hydraulics. Journal of Glaciology 53 (181), 257–265.

Brennand, T.A., 1994. Macroforms, large bedforms and rhythmic sedimentary sequences in subglacial eskers, south-central Ontario: implications for esker genesis and meltwater regime. Sedimentary Geology 91, 9–55.

Brennand, T.A., 2000. Deglacial meltwater drainage and glaciodynamics: inferences from Laurentide eskers, Canada. Geomorphology 32, 263–293.

Brennand, T.A., Shaw, J., 1994. Tunnel channels and associated landforms, south-central Ontario: their implications for ice-sheet hydrology. Canadian Journal of Earth Science 31, 505–522.

Brennand, T.A., Shaw, J., 1996. The Harricana glaciofluvial complex, Abitibi region, Quebec: its genesis and implications for meltwater regime and ice-sheet dynamics. Sedimentary Geology 102, 221–262.

Brennand, T.A., Russell, H.A.J., Sharpe, D.R., 2006. Tunnel channel character and evolution in central southern Ontario. In: Knight, P.G. (Ed.), Glacier Science and Environmental Change. Blackwell Publishing Ltd, Oxford, pp. 37–39.

Bretz, J.H., 1932. The Grand Coulee. In: American Geographical Society Special Publication 15. American Geographical Society, New York.

Burke, M.J., Brennand, T.A., Perkins, A.J. Transient subglacial hydrology of a thin ice sheet: insights from the Chasm esker, British Columbia, Canada. Quaternary Science Reviews, JQSR-D-12-00184, submitted for publication.

Burke, M.J., Woodward, J., Russell, A.J., Fleisher, P.J., 2009. Structural control on englacial esker sedimentation: Skeiðarárjökull, Iceland. Annals of Glaciology 50 (51), 85–92.

Burke, M.J., Woodward, J., Russell, A.J., Fleisher, P.J., Bailey, P.K., 2008. Controls on the sedimentary architecture of a single event englacial esker: Skeiðarárjökull, Iceland. Quaternary Science Reviews 27, 1829–1847.

Burke, M.J., Woodward, J., Russell, A.J., Fleisher, P.J., Bailey, P.K., 2010. The sedimentary architecture of outburst flood eskers: a comparison of ground-penetrating radar data from Bering Glacier, Alaska and Skeiðarárjökull, Iceland. Geological Society of America Bulletin 122, 1637–1645.

Campbell, R.B., Tipper, H.W., 1971. "A" series map 1278A (1:250,000). Geological Survey of Canada. http://dx.doi.org/10.4095/100369.

Carter, S.P., Blankenship, D.D., Young, D.A., Peters, M.E., Holt, J.W., Siegert, M.J., 2009. Dynamic distributed drainage implied by the flow evolution of the 1996–1998 adventure trench subglacial lake discharge. Earth and Planetary Science Letters 283, 24–37.

Clague, J.J., James, T.S., 2002. History and isostatic effects of the last ice sheet in southern British Columbia. Quaternary Science Reviews 21, 71–87.

Das, S.B., Joughin, I., Behn, M.D., Howat, I.M., King, M.A., Lizarralde, D., Bhatia, M., 2008. Fracture propagation to the base of the Greenland Ice Sheet during supraglacial lake drainage. Science 320, 778–781.

Denton, G.H., Sugden, D.E., 2005. Meltwater features that suggest Miocene ice-sheet overriding of the Transantarctic Mountains in Victoria Land, Antarctica. Geografiska Annaler 87, 67–85.

Ékes, C., Hickin, E., 2001. Ground penetrating radar facies of the paraglacial Cheekye fan, southwestern British Columbia, Canada. Sedimentary Geology 143, 199–217.

Fiore, J., Pugin, A., Beres, M., 2002. Sedimentological and GPR studies of subglacial deposits in the Joux Valley (Vaud, Switzerland): backset accretion in an esker followed by an erosive GLOF. Géographie physique et Quaternaire 56 (1), 19–32.

Fisher, T.G., Jol, H.M., Boudreau, A.M., 2005. Saginaw lobe tunnel channels (Laurentide Ice Sheet) and their significance in south-central Michigan, USA. Quaternary Science Reviews 24, 2375–2391.

Fountain, A.G., Walder, J.S., 1998. Water flow through glaciers. Reviews of Geophysics 36, 299–328.

Fricker, H.A., Scambos, T., 2009. Connected subglacial lake activity on lower Mercer and Whillans Ice Streams, West Antarctica, 2003–2008. Journal of Glaciology 55 (190), 303–315.

Fricker, H.A., Scambos, T., Bindschadler, R., Padman, L., 2007. An active subglacial water system in West Antarctica mapped from space. Science 315, 1544–1548.

Fulton, R.J., 1991. A conceptual model for the growth and decay of the Cordilleran Ice Sheet. Géographie Physique et Quaternaire 45 (3), 281–286.

Fulton, R.J., Smith, G.W., 1978. Late Pleistocene stratigraphy of south-central British Columbia. Canadian Journal of Earth Science 15, 971–980.

Goodwin, I.D., 1988. The nature and origin of a jökulhlaup near Casey Station, Antarctica. Journal of Glaciology 34, 95.

Gorrell, G., Shaw, J., 1991. Deposition in an esker, bead and fan complex, Lanark, Ontario, Canada. Sedimentary Geology 72, 285–314.

Gray, L., Joughin, I., Tulaczyk, S., Spikes, V.B., Bundschadler, R., Jezek, K., 2005. Evidence for subglacial water transport in the West Antarctic Ice Sheet through three-dimensional satellite radar interferometry. Geophysical Research Letters 32, L03501.

Heinz, J., Aigner, T., 2003. Three-dimensional GPR analysis of various Quaternary gravel-bed braided river deposits (southwestern Germany). In: Bristow, C.D., Jol, H.M. (Eds.), Ground Penetrating Radar in Sediments. Geological Society, London, Special Publications 211, pp. 99–110.

Huntley, D.H., Broster, B.E., 1994. Glacial Lake Camelsfoot: a Late Wisconsinan advance stage proglacial lake in the Fraser River Valley, Gang Ranch area, British Columbia. Canadian Journal of Earth Science 31, 798–807.

Huntley, D.H., Broster, B.E., 1996. The Late Wisconsinan deglacial history of the east-central Taseko Lakes area, British Columbia. Canadian Journal of Earth Science 34, 1510–1520.

Jordan, T.A., Ferraccioli, F., Corr, H., Graham, A., Armadillo, E., Bozzo, E., 2010. Hypothesis for mega-outburst flooding from a palaeo-subglacial lake beneath the East Antarctic Ice Sheet. Terra Nova 22, 283–289.

Jørgensen, F., Sandersen, P.B.E., 2008. Mapping of buried tunnel valleys in Denmark: new perspectives for the interpretation of the Quaternary succession. Geological Survey of Denmark and Greenland Bulletin 15, 33–36.

Krawczynski, M.J., Behn, M.D., Das, S.B., Joughin, I., 2009. Constraints on the lake volume required for hydro-fracture through ice sheets. Geophysical Research Letters 36, L10501.

Lang, J., Winsemann, J., Steinmetz, D., Pollok, L., Polom, U., Böhner, U., Serangeli, J., Brandes, C., Hampel, A., Winghart, S., 2012. The Pleistocene of Schöningen, Germany: a complex tunnel valley fill revealed from 3D subsurface modelling and shear wave seismics. Quaternary Science Reviews 39, 86–105.

Lesemann, J.-E., Brennand, T.A., 2009. Regional reconstruction of subglacial hydrology and glaciodynamic behaviour along the southern margin of the

Cordilleran Ice Sheet in British Columbia, Canada and northern Washington State, USA. Quaternary Science Reviews 28, 2420–2444.

Lesemann, J.-E., Piotrowski, J.A., Wysota, W., 2010. "Glacial curvilineations": new glacial landforms produced by longitudinal vortices in subglacial meltwater flow. Geomorphology 120, 153–161.

Lian, O.B., Hicock, S.R., 2000. Thermal conditions beneath parts of the last Cordilleran Ice Sheet near its centre as inferred from subglacial till, associated sediments, and bedrock. Quaternary International 68-71, 147–162.

Lian, O.B., Hicock, S.R., 2001. Lithostratigraphy and limiting optical ages of the Pleistocene fill in Fraser River valley near Clinton, south-central British Columbia. Canadian Journal of Earth Science 38, 839–850.

Mathews, W.H., 1989. Neogene Chilcotin basalts in south-central British Columbia: geology, ages, and geomorphic history. Canadian Journal of Earth Science 26, 969–982.

McMillan, M., Nienow, P., Shepherd, A., Benham, T., Sole, A., 2007. Seasonal evolution of supraglacial lakes on the Greenland Ice Sheet. Earth and Planetary Science Letters 262, 484–492.

Mooers, H.D., 1989. On the formation of the tunnel valleys of the Superior Lobe, central Minnesota. Quaternary Research 32, 24–35.

Neal, A., 2004. Ground-penetrating radar and its use in sedimentology: principles, problems and progress. Earth-Science Reviews 66, 261–330.

Ng, F.S.L., 2000. Canals under sediment-based ice sheets. Annals of Glaciology 30, 146–152.

Ó Cofaigh, C., 1996. Tunnel valley genesis. Progress in Physical Geography 20 (1), 1–19.

Palmer, S., Shepherd, A., Nienow, P., Joughin, I., 2011. Seasonal speed up of the Greenland Ice Sheet linked to routing of surface water. Earth and Planetary Science Letters 302, 423–428.

Piotrowski, J.A., 1994. Tunnel-valley formation in northwest Germany – geology, mechanisms of formation and subglacial bed conditions for the Bornhöved tunnel valley. Sedimentary Geology 89, 107–141.

Plouffe, A., Bednarski, J.M., Huscroft, C.A., Anderson, R.G., McCuaig, S.J., 2011. Late Wisconsinan glacial history in the Bonaparte Lake map area, south-central British Columbia: implications for glacial transport and mineral exploration. Canadian Journal of Earth Science 48, 1091–1111.

Province of British Columbia, 2010. 1 metre Resolution Black and White Orthophoto Mosaic (92Psw), 1:20,000. Open Government Licence for Government of BC information, vBC1.0.

Pugin, A., Pullan, S.E., Sharpe, D.R., 1999. Seismic facies and regional architecture of the Oak Ridges Moraine area, southern Ontario. Canadian Journal of Earth Science 36, 409–432.

Rampton, V.N., 2000. Large-scale effects of subglacial meltwater flow in the southern Slave Province, Northwest Territories, Canada. Canadian Journal of Earth Science 37, 81–93.

Rice, S.P., Church, M., Wooldridge, C.L., Hickin, E.J., 2009. Morphology and evolution of bars in a wandering gravel-bed river; lower Fraser river, British Columbia, Canada. Sedimentology 56, 709–736.

Roberts, M.J., 2005. Jökulhlaups: a reassessment of floodwater flow through glaciers. Reviews of Geophysics 43, RG1002.

Russell, H.A.J., Arnott, R.W.C., Sharpe, D.R., 2003. Evidence for rapid sedimentation in a tunnel channel, Oak Ridges Moraine, southern Ontario, Canada. Sedimentary Geology 160, 33–55.

Russell, A.J., Gregory, A.R., Large, A.R.G., Fleisher, P.J., Harris, T.D., 2007. Tunnel channel formation during the November 1996 jökulhlaup, Skeiðarárjökull, Iceland. Annals of Glaciology 45, 95–103.

Russell, A.J., Knudsen, Ó., Fay, H., Marren, P.M., Heinz, J., Tronicke, J., 2001. Morphology and sedimentology of a giant supraglacial, ice-walled, jökulhlaup channel Skeiðarárjökull, Iceland: implications for esker genesis. Global and Planetary Change 28, 193–216.

Shaw, J., 1983. Drumlin formation related to inverted melt-water erosional marks. Journal of Glaciology 29 (103), 461–479.

Shaw, J., Gorrell, G.A., 1991. Subglacially formed dunes with bimodal and graded gravel in the Trenton drumlin field, Ontario, Canada. Géographie Physique et Quaternaire 45, 21–34.

Sjogren, D.B., Fisher, T.G., Taylor, L.D., Jol, H.M., Munro-Stasiuk, M.J., 2002. Incipient tunnel channels. Quaternary International 90, 41–56.

Sole, A.J., Mair, D.W.F., Nienow, P.W., Bartholemew, I.D., King, M.A., Burke, M.J., Joughin, I., 2011. Seasonal speed-up of a Greenland marine-terminating outlet glacier forced by surface melt-induced changes in subglacial hydrology. Journal of Geophysical Research 116, F03014.

Stearns, L.A., Smith, B.E., Hamilton, G.S., 2008. Increased flow speed on a large East Antarctic outlet glacier caused by subglacial floods. Nature Geoscience 1, 827–831.

Stokes, C.R., Clark, C.D., Lian, O.B., Tulaczyk, S., 2007. Ice stream sticky spots: a review of their identification and influence beneath contemporary and palaeo-ice streams. Earth-Science Reviews 81, 217–249.

Stokes, C.R., Lian, O.B., Tulaczyk, S., Clark, C.D., 2008. Superimposition of ribbed moraines on a palaeo-ice-stream bed: implications for ice stream dynamics and shutdown. Earth Surface Processes and Landforms 33, 593–609.

Sundal, A., Shepherd, A., Nienow, P., Hanna, E., Palmer, S., Huybrechts, P., 2011. Melt induced speed-up of Greenland Ice Sheet offset by efficient subglacial drainage. Nature 469, 521–524.

Tipper, H.W., 1971. Multiple glaciation in central British Columbia. Canadian Journal of Earth Sciences 8, 743–752.

Tweed, F.S., Russell, A.J., 1999. Controls on the formation and sudden drainage of glacier-impounded lakes: implications for jökulhlaups characteristics. Progress in Physical Geography 23 (1), 90–110.

Utting, D.J., Ward, B.C., Little, E.C., 2009. Genesis of hummocks in glaciofluvial corridors near the Keewatin Ice Divide, Canada. Boreas 38, 471–481.

Van Dam, R.L., 2012. Landform characterization using geophysics – recent advances, applications, and emerging tools. Geomorphology 137, 57–73.

Walder, J.S., Fowler, A., 1994. Channelized subglacial drainage over a deformable bed. Journal of Glaciology 40 (134), 3–15.

Wingfield, R., 1990. The origin of major incisions within the Pleistocene deposits of the North Sea. Marine Geology 91, 31–52.

Wingham, D.J., Siegert, M.J., Shepherd, A., Muir, A.S., 2006. Rapid discharge connects Antarctic subglacial lakes. Nature 440, 1033–1036.

Woodward, J., Burke, M.J., Tinsley, R., Russell, A.J., 2008. Investigating reworking of proglacial sediments using GPR: Skeiðarárjökull, Iceland. In: Rodgers, C.D.F., Chignell, R.J. (Eds.), Proceedings of the 12th International Conference on Ground Penetrating Radar. University of Birmingham, Birmingham.

Wright, H.E., 1973. Tunnel valleys, glacial surges and subglacial hydrology of the superior lobe, Minnesota. In: Black, R.F., Goldthwaite, R.P., Willman, H.B. (Eds.), The Wisconsinan Stage. Memoir 136, vol. 136. Geological Society of America, Boulder, pp. 251–276.

Wright, A., Siegert, M.J., 2011. The identification and physiographical settings of Antarctic subglacial lakes: an update based on recent discoveries. In: Siegert, M.J., Kennicutt, I.I.M.C., Bindschadler, R.A. (Eds.), Antarctic Subglacial and Aquatic Environments. Geophysical Monograph 192. Geopress, American Geophysical Union, Washington, DC, pp. 9–26.

Zwally, H.J., Abdalati, W., Herring, T., Larson, K., Saba, J., Steffen, K., 2002. Surface melt-induced acceleration of Greenland Ice-Sheet flow. Science 297, 218–222.